Side-to-Face Ruthenium Porphyrin Arrays: Photophysical Behavior of Dimeric and Pentameric Systems

Anna Prodi,[a] Maria Teresa Indelli,[a] Cornelis J. Kleverlaan,[a] Franco Scandola,*[a] Enzo Alessio,[b] Teresa Gianferrara,[c] and Luigi G. Marzilli[d]

Abstract: The investigated systems are side-to-face porphyrin arrays made of two types of molecular components: a porphyrin unit with *meso*-pyridyl substituents, and one or more ruthenium carbonyl tetraphenylporphyrin units. The two types of unit are assembled by axial coordination of the *meso*-pyridyl groups of the former onto the metal center of the latter. The number (one or four) of the *meso*-pyridyl groups on the axial unit determines whether the arrays are dimeric or pentameric. The geometry of the groups (4′-pyridyl or 3′-pyridyl) determine whether the arrays have perpendicular or canted structures. Furthermore, the *meso*-pyridyl porphyrin can be either free-base or zinc-substituted, leading to a total of eight different arrays. All arrays were shown to be stable in toluene, even in the dilute solutions (1×10^{-5} M) required for photophysical experiments. The energy levels of the molecular components are practically unaltered in the arrays, with the excited states of the ruthenium porphyrin units always higher, both at the singlet and the triplet level, than those of the free-base or zinc porphyrin units. The photophysical behavior of the arrays has been studied in detail. The behavior was found to be practically independent of the perpendicular or canted nature of the systems. The arrays exhibit two main supramolecular features, distinctive with respect to the behavior of the monomeric molecular components (or suitable models thereof). At the singlet level, the behavior of the ruthenium unit is normal (100% efficient intersystem crossing to the triplet state) but that of the axial unit is strongly perturbed, as indicated by pronounced fluorescence quenching. This effect is attributed to enhanced intersystem crossing in the free-base or zinc porphyrin unit, owing to the heavy-atom effect provided by the attached ruthenium units. At the triplet level, efficient energy transfer between the units takes place. When the axial unit is a free-base porphyrin, the driving force is large, and the process takes place irreversibly from the ruthenium to the free-base triplet. When the axial unit is a zinc porphyrin, the energy difference between the triplet states is small, and an equilibrium between the two states is established prior to deactivation. In the free-base systems, triplet energy transfer rate constants are found to be in the $10^8-10^9\ s^{-1}$ range.

Keywords: energy transfer · photochemistry · porphyrin arrays · supramolecular chemistry

Introduction

Because of their key role in many important biological systems, porphyrins and metallo-porphyrins[1] are molecular species of great chemical interest. Such species also occupy a relevant position in the rapidly developing field of supramolecular chemistry,[2] since they are frequently used as building blocks for the construction of artificial systems with special built-in properties or functions. Remarkable examples include the supramolecular systems designed to feature a number of light-induced functions,[3] notably those inspired by natural photosynthesis. Photoinduced charge separation in the reaction center[4–8] is mimicked by several types of covalently linked donor–acceptor systems, including triads and more complex architectures.[9–11] Synthetic multi-porphyrin arrays are suitable model systems for the light-harvesting function performed by a large number of chlorophyll molecules in antenna units.[12–15]

Various type of connecting motifs can be used to construct porphyrin arrays. Side-by-side connection involves the formation of covalent links between porphyrin rings (usually at *meso* positions). Side-to-face connection is obtained when a porphyrin carrying suitable peripheral Lewis-base functions (usually as substituents at *meso* positions) binds, by means of

[a] Prof. F. Scandola, A. Prodi, Dr. M. T. Indelli, Dr. C. J. Kleverlaan
Dipartimento di Chimica, Università di Ferrara, Centro di Fotoreattività e Catalisi CNR
Via L. Borsari 46, I-44100 Ferrara (Italy)
Fax: (+39) 532-240709
E-mail: snf@dns.unife.it

[b] Dr. E. Alessio
Dipartimento di Scienze Chimiche, Universita′ di Trieste I-34127 Trieste (Italy)

[c] Dr. T. Gianferrara
Dipartimento di Scienze Farmaceutiche, Università di Trieste, I-34127 Trieste (Italy)

[d] Prof. L. G. Marzilli
Department of Chemistry, Emory University
Atlanta, GA 30323 (USA)

0947-6539/99/0509-2668 $ 17.50+.50/0 *Chem. Eur. J.* **1999**, *5*, No. 9

axial coordination, to the metal of a second porphyrin. By the use of these and other connecting motifs, a large variety of multi-porphyrin systems of different shape and function have been produced in recent years.[16–27] Notable examples of light-harvesting systems are pentameric arrays made of a central free-base porphyrin and four peripheral Zn porphyrins.[18c, 19c, 24, 25] In some such systems, the central unit is laterally connected, in a starlike geometry, to four peripheral Zn porphyrins.[24, 25] In other cases, the four peripheral Zn porphyrin units are linked side-by-side to form a cyclic square box-type cavity, where a central *meso*-tetrapyridyl free-base porphyrin is hosted in a side-to-face arrangement.[18c, 19c] In these Zn/free-base systems, the antenna effect is obtained by very efficient singlet–singlet energy transfer which conveys the excitation energy from the peripheral chromophores to the central one.

In one of our laboratories, a series of stable and inert side-to-face perpendicular arrays has been produced with free-base or zinc 4′-pyridylporphyrins and ruthenium porphyrins.[28] The dimeric [Ru(TPP)(CO)(4′MPyP)] and pentameric (4′TPyP)[Ru(TPP)(CO)]$_4$ (abbreviations are given in ref. [29]) free-base species, thereafter designated as **Fb(4)Ru** and **Fb(4)Ru$_4$**, are represented schematically in Figure 1. Analogous species that contain a Zn center instead of free-base porphyrin are designated **Zn(4)Ru** and **Zn(4)Ru$_4$**. In order to check possible effects of the mutual orientation of the porphyrin rings, an analogous series of canted side-to-face arrays was recently synthesized[30] with 3′-pyridyl substituents as connecting groups. The dimeric free-base species [Ru(TPP)(CO)(3′MPyP)] (**Fb(3)Ru**) is shown in Figure 1. The analogous pentameric species (3′TPyP)[Ru(TPP)(CO)]$_4$ (**Fb(3)Ru$_4$**) is not depicted in Figure 1 for practical reasons. The crystal structure of the Zn derivative shows that it has a flying saucer shape, with peripheral ruthenium porphyrin units alternately above and below the plane of the free-base porphyrin, and angles between central and peripheral porphyrin rings of close to 40°.[30] Related side-to-face arrays based on ruthenium and osmium octaethyl porphyrins have also been recently synthesized.[31]

With respect to previously investigated pentameric light-harvesting arrays that contain Zn and free-base porphyrins,[18c, 19c, 24, 25] the systems in Figure 1 are expected to have similar excited-state energy ordering. This means that the excited states of the peripheral units will be higher than those of the central unit. In this case, however, the presence of the heavy metal is likely to promote very efficient intersystem crossing in the Ru-containing porphyrin units,[32] which makes these systems suitable for the study of intercomponent energy transfer at the *triplet*, rather than at the singlet level. Here we present a detailed study of the photophysical behavior of the perpendicular and canted arrays.

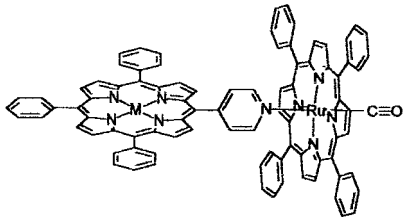

M = 2H$^+$, Fb(4)Ru
M = Zn, Zn(4)Ru

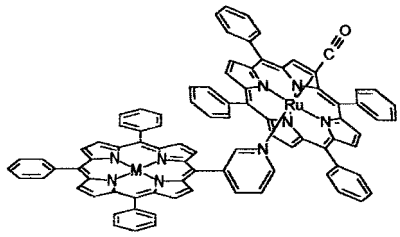

M = 2H$^+$, Fb(3)Ru
M = Zn, Zn(3)Ru

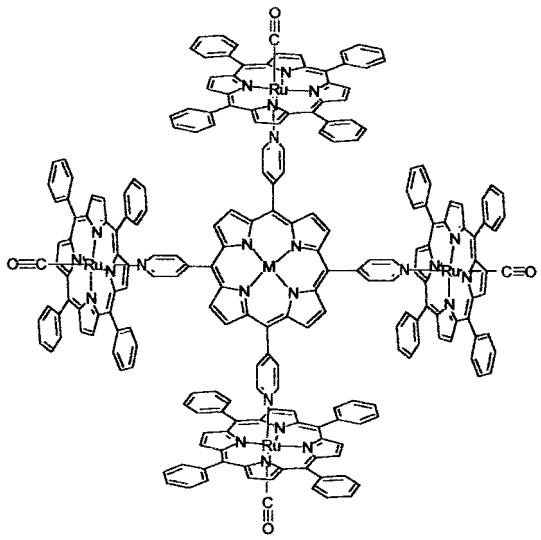

M = 2H$^+$, Fb(4)Ru$_4$
M = Zn, Zn(4)Ru$_4$

Figure 1. Schematic structures of the dimeric and pentameric species, and definition of the shorthand notations used throughout the paper. For practical reasons, the *meso* phenyl groups are depicted as coplanar, although they are in reality almost perpendicular to the porphyrin rings. The structures of the pentameric species **Fb(3)Ru$_4$** and **Zn(3)Ru$_4$** (not shown in the figure for practical reasons) can easily be deduced from that of the corresponding dimeric species.

Results and Discussion

Stability in solution: The key to the stability of side-to-face arrays is the strength of the coordinative bond between the pyridyl group of the side porphyrin and the metal of the face porphyrin. For example, when the metal is Zn, the coordinative bond is intrinsically weak. Thus, coordination polymers are often generated,[33] but stable arrays of well-defined stoichiometry are difficult to obtain in solution unless the coordination is spatially enforced (e.g. when the side porphyrin is bound as a guest into a cyclic host of face metal porphyrins).[18c, 19c] From this viewpoint, Ru-based arrays are expected to be intrinsically more stable. Thus, dimeric and pentameric arrays of the type studied in this work can easily self-assemble and be isolated as solid products.[28, 30, 31] In some instances, the structure can be obtained from X-ray crystallo-

graphic data.[30] In all cases, highly diagnostic ^{1}H NMR spectra demonstrate that the stoichiometry and structure of the arrays is maintained in $CHCl_3$.[28, 30, 31] A word of caution is worthwhile, however, with regard to stability for this type of systems in solution.[34] It should be stressed that NMR spectroscopic data are normally obtained at much higher concentrations than those usually required for photophysical studies ($\approx 10^{-5}$ M), and that structural information from NMR data cannot be obviously extrapolated to such highly diluted conditions. Independent proof of the stability of the arrays in dilute solution is needed, although this is not a trivial problem.

For arrays of this type, stability is likely to depend critically on the solvent. A coordinating solvent may compete with the pyridyl groups for the metal of the Ru(TPP)(CO) fragment, favoring dissociation of the arrays. In this regard, the relevant solvent parameter is expected to be the donor number (DN), given the general correlation between the stability of Ru(TPP)(CO)(X) adducts and the DN of the axial ligand X.[35] This was confirmed by screening carried out on the stability of the arrays in various solvents, as a function of dilution. In DMF (DN = 26.6), the ^{1}H NMR spectrum of **Fb(4)Ru$_4$** showed complex patterns which indicate that substantial dissociation takes place already at a concentration of 3×10^{-4} M. On the other hand, in $CHCl_3$ (DN $\approx$ 0), the simple ^{1}H NMR pattern characteristic of the highly symmetric **Fb(4)Ru$_4$** pentamer[28] was maintained in solutions as dilute as 5×10^{-5} M (lowest experimental limit). At concentrations below 3×10^{-5} M, however, some dissociation was found to take place even in this solvent, as indicated by small visible spectral changes (slight blue shift of the 531 nm band). Thus, $CHCl_3$ is a much better solvent than DMF for these arrays, but still presents some problems in highly dilute solution. After further solvent screening, the best choice proved to be toluene (DN $\approx$ 0), in which no dissociation of **Fb(4)Ru$_4$** upon dilution could be detected spectrophotometrically down to at least 5×10^{-6} M.

All the arrays (dimers or pentamers, free-base or Zn-substituted, with 3′-pyridyl or 4′-pyridyl linkages) were found to behave similarly with respect to stability in solution. This preliminary study was useful for the definition of the experimental conditions to be used in the subsequent photophysical work. Unless otherwise noted, all the experiments reported in the following sections refer to $\geq 1 \times 10^{-5}$ M solutions in toluene. Under these conditions, the arrays are definitely intact in solution. This is demonstrated by the photophysical results discussed below which always proved to be independent on array concentration in the range $1-5 \times 10^{-5}$ M.

Monomeric model systems: The arrays are made up of two types of molecular components, which are generally ruthenium porphyrin units and free-base (or zinc-substituted) porphyrin units. In order to discuss the photophysical behavior of the arrays, it is useful to have simple molecular systems that model the intrinsic behavior of such molecular components.

For the ruthenium porphyrin units, a model molecule that reproduces the metal coordination environment of the arrays very closely is Ru(TPP)(CO)py (**Ru**). For the free-base units, the choice was obvious, as 4′MpyP, 4′TpyP, 3′MpyP, and 3′TPyP[29] are directly available as molecular species. In practice, the photophysical behavior of all these monomeric free-base species was found to be very similar; the differences between various species being limited to minor shifts (± 2 nm) in emission maxima and minor changes (± 2 ns) in emission lifetime. Thus, 4′MpyP (**Fb**) was used as a general model for all the free-base molecular components. For the zinc porphyrin units, similar arguments can be used to justify the use of a single model for all the arrays. In this case, however, given the tendency of zinc pyridylporphyrin systems to self-associate,[33a] the tetraphenyl analogue ZnTPP[29] (**Zn**) was used as a model. The photophysical behavior of the **Ru**, **Fb**, and **Zn** model systems is described below in some detail.

Fb: This model exhibited straightforward behavior, typical of free-base porphyrins.[36] The absorption spectrum (Figure 2a) exhibited the typical pattern with four Q-bands in addition to

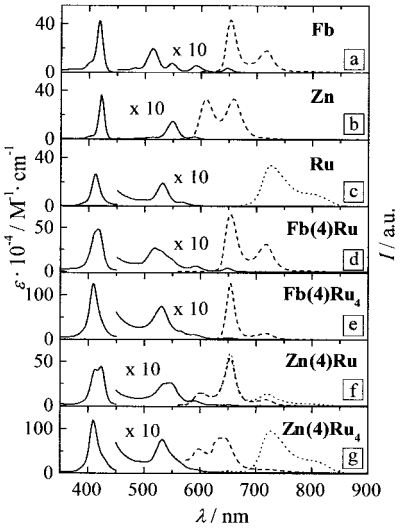

Figure 2. Absorption and emission spectra of porphyrin arrays and monomeric models in toluene solution. Absorption: ——. Emission: aerated, - - - -; deaerated, ····; $\lambda_{exc} = 530$ nm.

the Soret band. The emission (Figure 2a) is fluorescence from the lowest singlet $\pi-\pi^*$ state, ^{1}*Fb, with the 0–0 and 0–1 transition at 653 and 717 nm. The emission is practically oxygen-independent,[37] with a lifetime of 9.7 ns in aerated toluene solution. Based on values measured for the tetraphenyl and tetrapyridyl analogues,[38] the fluorescence quantum yield is presumably about 0.1 and that for formation of the triplet state is about 0.9. The lowest $\pi-\pi^*$ triplet, ^{3}*Fb (estimated energy of 1.44 eV[36]), is non-emissive, both at room temperature and at 77 K. It can be easily monitored at room temperature, in deaerated solutions, by transient absorption in laser flash photolysis ($\lambda_{max} \leq 440$ nm, Figure 3). The triplet decays with mixed first-order/second-order kinetics (Figure 4), attributable to competition between unimolecular decay and triplet–triplet bimolecular annihilation processes.[36] At high laser power, the decay is dominated by the second-order annihilation process, with a rate constant close to the diffusion-controlled limit.[39] At very low power, the

0947-6539/99/0509-2670 $ 17.50+.50/0 Chem. Eur. J. 1999, 5, No. 9

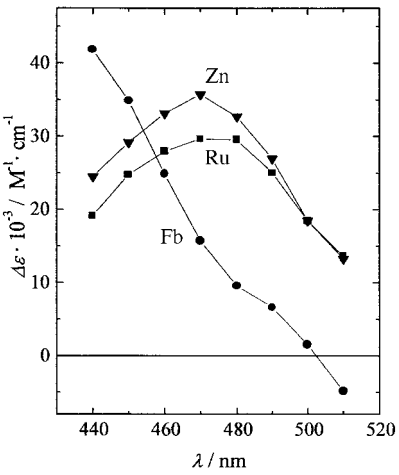

Figure 3. Transient absorption spectra obtained for **Fb** (●), **Ru** (■), and **Zn** (▼). Deaerated solution in toluene; 532 nm pulsed excitation; delay from laser pulse 15 ns.

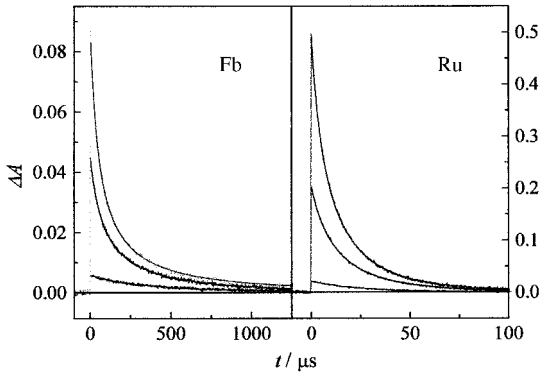

Figure 4. Transient absorbance decays for **Fb** and **Ru** in deaerated toluene solution, monitored at 460 nm at different laser intensities (intensity decreasing from upper to lower trace, 6.7, 0.7, 0.1 mJ per pulse; sample concentration, 1×10^{-5} M).

decay becomes appreciably first-order, to yield a lifetime for the triplet state of 0.8 ms under our conditions. The photophysical behavior of the **Fb** model system is summarized in Figure 5.

Zn: The absorption spectrum (Figure 2b) shows the typical pattern of regular metal porphyrins[36] with two Q-bands in addition to the Soret band. The photophysics of **Zn** is qualitatively similar to that of **Fb**. The fluorescent emission is blue-shifted (0–0 and 0–1 band at 609 nm and 658 nm) with respect to **Fb**, and has a somewhat different profile (0–1 stronger than 0–0), and a shorter lifetime, 2.4 ns. Quantum yields of fluorescence and triplet formation are presumably similar to those measured in other solvents (0.04 and 0.88, respectively).[36] The ^{3}*Zn triplet state is practically non-emissive ($\Phi \approx 10^{-4}$) at room temperature, although a distinct phosphorescent emission at 783 nm can be observed at 77 K (Figure 6). In deaerated solutions at room temperature, ^{3}*Zn

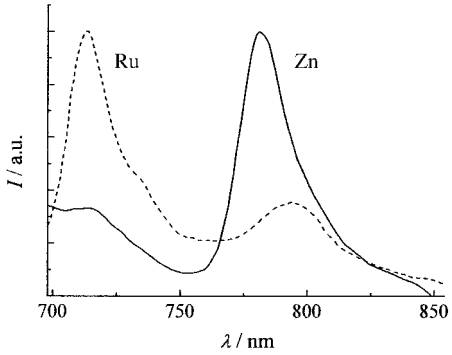

Figure 6. Emission spectra (arbitrary units) at 77 K of **Zn** (——) and **Ru** (- - - -) in a 4/1 EtOH/MeOH matrix.

can be easily monitored by transient absorption in laser flash photolysis ($\lambda_{max} = 470$ nm, Figure 3). It decays with mixed first-order/second-order kinetics,[39] again attributable to competition between unimolecular decay and triplet–triplet bimolecular annihilation. At very low laser power, the decay becomes appreciably first-order, to yield a lifetime for the triplet state of 0.9 ms under our experimental conditions. The photophysical behavior of the **Zn** model system is summarized in Figure 5.

Ru: The absorption spectrum is shown in Figure 2c. The emission observed in deaerated solution ($\lambda_{max} = 726$ nm) is also shown in Figure 2c. It is weak ($\Phi \approx 10^{-3}$) and strongly red-shifted with respect to the lowest energy absorption band. Its decay is complex (although the emission is too weak for detailed kinetic fits) and takes place on the microsecond time scale. The emission is completely quenched in aerated solutions. All these features indicate that the emission is phosphorescence from the lowest triplet state ^{3}*Ru. The phosphorescence spectrum does not change at 77 K, except for a small blue shift and band narrowing (Figure 6). In **Ru**, the lack of fluorescence and the appearance of phosphorescence at room temperature are consequences of the strong spin-orbit coupling provided

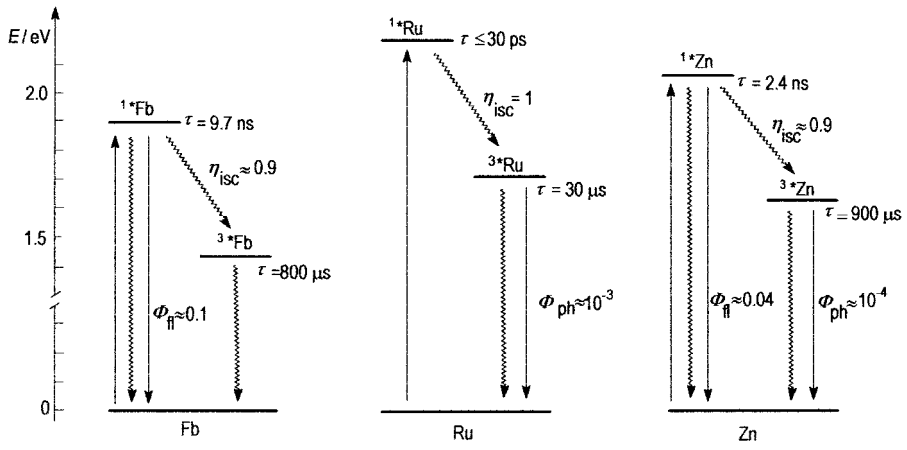

Figure 5. Energy levels and summary of photophysical behavior of the monomeric model systems.

by the heavy metal, which leads to very fast[32] ^{1}*Ru $\rightarrow$ ^{3}*Ru intersystem crossing and a relatively large ^{3}*Ru $\rightarrow$ Ru radiative rate constant. The triplet state can be conveniently monitored at room temperature, in laser flash photolysis of deaerated solutions, by transient absorption ($x_{max} = 470$ nm, Figure 3). The triplet decays with mixed first-order/second-order kinetics (Figure 4),[39] attributable to competition between unimolecular decay and triplet–triplet bimolecular annihilation processes. At high laser power, the decay is dominated by the second-order annihilation process, with a rate constant close to the diffusion-controlled limit. At very low power, the decay becomes appreciably first-order, to yield a lifetime for the triplet state of 30 μs. The photophysical behavior of **Ru** model system is summarized in Figure 5. Upon prolonged laser irradiation, some photochemical decomposition of the samples was observed. Photodissociation of CO from **Ru** has been reported,[32] with a quantum yield of $\approx 10^{-4}$ in neat pyridine. In the conditions used here for flash photolysis (fresh solutions, small number of pulses or low power), photodecomposition was always negligible. The same is true for all the laser photolysis experiments described below for the various arrays.

Energy levels and intercomponent processes: The absorption spectra of a number of representative arrays in toluene are shown in Figure 2. In the visible region, the spectra of the arrays can always be reproduced (within ±10%) from a superposition of the spectra of the appropriate model compounds, as shown in Figure 7 for **Fb(4)Ru**. This additive

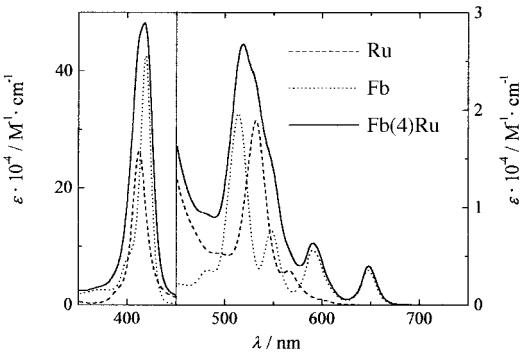

Figure 7. Comparison between the absorption spectra of **Fb(4)Ru** (——), **Fb** (·····), and **Ru** (- - - -) in toluene.

behavior supports a supramolecular view of the arrays. This picture is reinforced by results to be discussed in the next section, which show that i) the emissions from the molecular components in the arrays when observed always coincide in energy with those of the model systems, and that ii) the transient absorption spectra of the arrays always have maxima coincident with those of model systems. Overall, the good qualitative correspondence between the spectroscopic signatures of arrays and monomeric models, indicates that these arrays are true supramolecular systems (i.e. weakly interacting multicomponent systems in which the energy levels of each molecular component are substantially unperturbed by intercomponent interactions).[3a]

Thus, the energy-level diagrams of the model compounds (Figure 5) can be simply added together to construct energy-level diagrams for the dimeric and pentameric systems. Given the supramolecular nature of the species investigated and the negligible differences between the various free-base porphyrins, a single energy-level diagram (Figure 8) should be appropriate for **Fb(4)Ru**, **Fb(3)Ru**, **Fb(4)Ru$_4$**, and **Fb(3)Ru$_4$**. Similarly, a single energy-level diagram (Figure 9) is appropriate for **Zn(4)Ru**, **Zn(3)Ru**, **Zn(4)Ru$_4$**, and **Zn(3)Ru$_4$**. It should be recalled that the complete energy-level diagram of a supramolecular system should include, in addition to the local excited states of the molecular components, intercomponent electron transfer states. From the electrochemistry of the **Fb**,[31b] **Ru**,[40] and **Zn**[41] models, a relatively low-energy charge transfer state is expected in the arrays, corresponding to oxidation of the ruthenium porphyrin and reduction of the attached unit. An estimate of the energy of such a charge transfer state requires knowledge of the redox potentials for the first oxidation and reduction of the arrays. For the free-base systems, these potentials have been measured, in CH_2Cl_2 vs. SCE, as +0.84 V and −1.17 V for **Fb(4)Ru** and +0.86 V

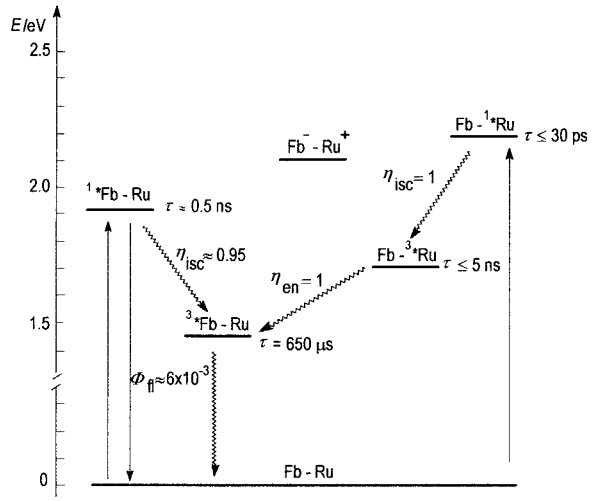

Figure 8. Energy-level diagram for the arrays based on free-base porphyrins **Fb(4)Ru**, **Fb(3)Ru**, **Fb(4)Ru$_4$**, and **Fb(3)Ru$_4$**. The photophysical parameters are those of **Fb(4)Ru$_4$** (for **Fb(4)Ru**, see Table 1).

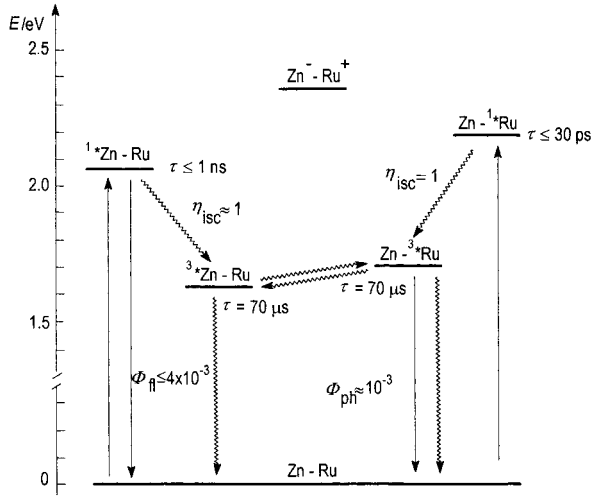

Figure 9. Energy-level diagram for the arrays based on zinc porphyrins **Zn(4)Ru**, **Zn(3)Ru**, **Zn(4)Ru$_4$**, and **Zn(3)Ru$_4$**. The photophysical parameters are those of **Zn(4)Ru$_4$** (for **Zn(4)Ru**, see Table 1).

0947-6539/99/0509-2672 $ 17.50+.50/0 *Chem. Eur. J.* **1999**, *5*, No. 9

(four-electron wave) and −0.96 V for **Fb(4)Ru$_4$**. From these data, the energy of the charge transfer state can be estimated[42, 43] as about 2.28 eV for **Fb(4)Ru** and 2.10 eV for **Fb(4)Ru$_4$**. Given the general cathodic shift of about 0.25 V for the reduction of zinc porphyrins with respect to free-base analogues,[41] the corresponding values for **Zn(4)Ru** and **Zn(4)Ru$_4$** should be about 2.53 eV and 2.35 eV.

The supramolecular description sketched above implies that energy levels and many of the intrinsic properties of the molecular components are maintained within the arrays. This does not mean, however, that the photophysical behavior of the arrays is simply a superposition of that of the components. Two factors can make the behavior of the arrays different from that of the molecular components: (i) even a small intercomponent perturbation can, in some cases, lead to sizeable changes in the kinetics of *intra*component photophysical processes; (ii) new, *inter*component energy or electron transfer processes may occur. On the basis of the energy-level diagrams in Figures 8 and 9, a number of thermodynamically allowed intercomponent processes can be identified for the various arrays. Using a condensed shorthand notation in which Fb-Ru and Zn-Ru denote the various arrays (regardless of whether they are dimeric or pentameric systems, and of whether they contain 3′-pyridyl- or 4′-pyridyl- linkages), the thermodynamically allowed processes are given in Equations (1)–(5).

$$\text{Fb-}^{1}\text{*Ru} \rightarrow {}^{1}\text{*Fb-Ru} \quad \textit{Ru} \rightarrow \textit{Fb singlet energy transfer} \tag{1}$$

$$\text{Fb-}^{1}\text{*Ru} \rightarrow \text{Fb}^{-}\text{-Ru}^{+} \quad \textit{Ru} \rightarrow \textit{Fb electron transfer} \tag{2}$$

$$\text{Fb-}^{3}\text{*Ru} \rightarrow {}^{3}\text{*Fb-Ru} \quad \textit{Ru} \rightarrow \textit{Fb triplet energy transfer} \tag{3}$$

$$\text{Zn-}^{1}\text{*Ru} \rightarrow {}^{1}\text{*Zn-Ru} \quad \textit{Ru} \rightarrow \textit{Zn singlet energy transfer} \tag{4}$$

$$\text{Zn-}^{3}\text{*Ru} \rightarrow {}^{3}\text{*Zn-Ru} \quad \textit{Ru} \rightarrow \textit{Zn triplet energy transfer} \tag{5}$$

In order to check for the occurrence of any of the above intercomponent processes, the ideal situation would be one that allows selective excitation of the two types of molecular component. This is not possible, at least for the ruthenium porphyrin units, because of spectral overlap. Nevertheless, the additive character (see above) of the spectra permits an accurate evaluation of the relative amount of exciting light absorbed, at any wavelength, by the various molecular components. For instance, 530 nm is a convenient wavelength for predominant excitation of the ruthenium porphyrin units, with calculated fractions of about 80% for the dimeric species and about 95% for the pentameric species (at 532 nm, the wavelength of the frequency doubled Nd/YAG laser, the same values apply). On the other hand, selective excitation (practically 100%) of the free-base and zinc porphyrin units can be achieved in the various arrays at $\lambda > 600$ nm and $\lambda > 570$ nm, respectively.

Singlet excited-state behavior: Since all triplet phenomena in the monomeric models are efficiently quenched by oxygen, the behavior of the arrays in aerated solution can only give information on processes that take place at the singlet level (Figures 8 and 9). The emission spectra of selected arrays in aerated solutions in toluene are shown in Figure 2. Comparison with the emission spectra of the model compounds shows that all the arrays exhibit exclusively fluorescence from the axial, free-base or zinc, porphyrin unit. This is expected from the properties of the molecular components (see above) and indicates that the ruthenium porphyrin units are intrinsically non fluorescent.

Given the energy-level diagrams in Figures 8 and 9, the fluorescence from the axial porphyrin unit could, in principle, arise not only from direct excitation of such units but also from singlet energy transfer from the ruthenium units [Eq. (1) and (4)]. This does *not* take place, however, as demonstrated by fluorescence excitation spectra. The fluorescence excitation spectrum of **Fb(4)Ru$_4$** is reported as an example (Figure 10) to show the complete lack of ruthenium porphyrin

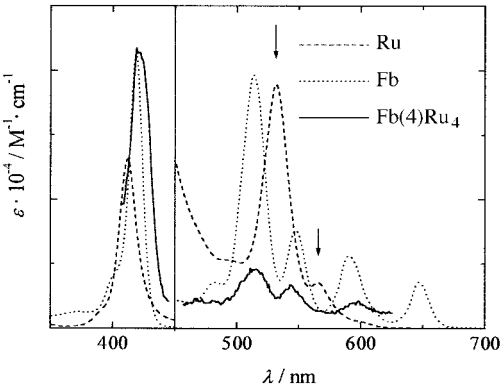

Figure 10. Fluorescence excitation spectrum of **Fb(4)Ru$_4$** in toluene (——, $\lambda_{em} = 654$ nm), compared with the absorption spectra of **Fb** (·····) and **Ru** (- - - -).

absorption features (that dominate the array absorption spectrum) and the close correspondence to the absorption spectrum of **Fb**. The most likely reason for the lack of energy transfer at the singlet level is the exceedingly short lifetime of the ruthenium porphyrin singlet (<30 ps for **Ru**).[32] It is known that singlet energy transfer in covalently linked porphyrins, especially when assisted by through-bond interactions, can have rates in the 10–100 ps time domain.[25b, 44] Evidently, in the present systems, singlet energy transfer [Eq. (1) and (4)] is not fast enough to compete with intersystem crossing in the ruthenium unit (Fb-^{1}*Ru → Fb-^{3}*Ru, Figure 8). In principle, competitive quenching of the ruthenium singlet by electron transfer [Eq. (2)] could be considered as an alternative reason for the observed lack of sensitization of free-base fluorescence. This possibility is ruled out, however, by the observation (see below) that the efficiency of intersystem crossing in the ruthenium unit (in Figure 8, Fb-^{1}*Ru → Fb-^{3}*Ru) is unitary in all arrays. It should be pointed out that similar behavior (i.e. lack of sensitized fluorescence of the central porphyrin by the peripheral units) was observed in a related system where a free-base pyridylporphyrin is coordinated to four peripheral ruthenium polypyridine units.[45]

Interestingly, the fluorescence that originates from direct excitation of the free-base or zinc porphyrin units in the arrays is definitely weaker than that of the corresponding monomeric model systems. This is shown in Figure 11 for **Fb**,

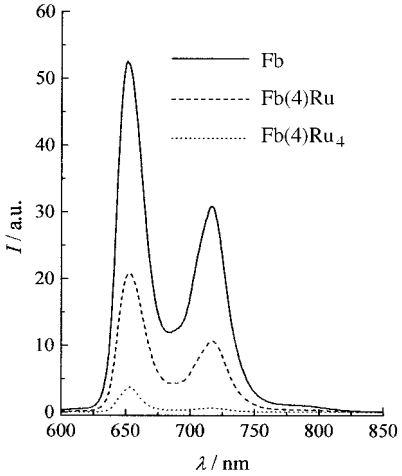

Figure 11. Fluorescence spectra of **Fb**, **Fb(4)Ru**, and **Fb(4)Ru$_4$** (λ_{ex} = 588 nm; optically matched solutions).

Fb(4)Ru, and **Fb(4)Ru$_4$** solutions, optically matched at 588 nm, where the free-base is the only light-absorbing unit. The relative fluorescence intensities are reported in Table 1, together with analogous data for the zinc-substituted series **Zn**, **Zn(4)Ru**, and **Zn(4)Ru$_4$** (solutions optically matched at 588 nm, where the zinc porphyrin is the only light-absorbing unit). The decrease in fluorescence intensity was accompanied, as expected, by a parallel decrease in fluorescence lifetime (Table 1). Thus, the general behavior is that the free-base and zinc porphyrin units become less emitting and shorter lived upon array formation. In some dyads and arrays with zinc and free-base porphyrins,[18c, 25b, 44] partial quenching of the lowest singlet state has been observed and attributed to interporphyrin electron transfer. In the present arrays, electron transfer states are definitely too high (Figures 8 and 9) to be directly involved in the quenching of the axial porphyrin singlet state. The fact that the effect persists in low-temperature rigid matrices (e.g. **Zn(4)Ru$_4$** remains practically non fluorescent at 77 K in methylcyclohexane) further rules out electron transfer as an explanation. The most likely explanation for this effect is the spin-orbit perturbation provided by the ruthenium centers (heavy-atom effect)[19e] which leads to enhanced intersystem crossing in the axial porphyrin (in Figure 8, ^{1}*Zn-Ru $\rightarrow$ ^{3}*Zn-Ru in Figure 9). The fact that, within a given series, the effect seems to increase with the number of ruthenium – porphyrin units in the array is in keeping with this hypothesis. The propagation of spin-orbit coupling within the arrays, from the heavy Ru unit onto the light Fb (or Zn) unit, probably depends on the degree of electron delocalization between these centers. A convenient way to represent this delocalization is by mixing the Fb^--Ru^+ and Zn^--Ru^+ electron transfer states into the local singlet states of the two units. From this point of view, the presence of relatively close-lying electron transfer states could play a relevant, though indirect, role in the observed effect. A reduction in fluorescence intensity of pyridyl porphyrins upon binding to heavy metal complex units has been reported in a number of other systems[19a,d,e] although, with one exception,[19e] its origin was not discussed.

For the sake of simplicity, the photophysical behavior at the singlet level has been described in detail for the arrays of the perpendicular type. Within the accuracy of our experiments, the behavior of the arrays of the canted series is practically indistinguishable from that of the corresponding perpendicular ones.

Triplet excited-state behavior: For the study of the behavior at the triplet level, work in carefully deaerated solution was required. As shown by the monomeric models, the following experimental handles are available for the study of the triplet states in the arrays: transient triplet absorption (for free-base, zinc, and ruthenium porphyrin), low-temperature phosphorescent emission (for zinc and ruthenium porphyrin), and room-temperature phosphorescence (for ruthenium porphyrin triplets). When applied to the arrays, the detection of phosphorescence from the ruthenium porphyrin at room temperature is expected to be complicated by the presence of overlapping (see Figures 2a – c) and intrinsically stronger free-base (or zinc porphyrin) fluorescence. This problem can be easily circumvented, however, by taking advantage of the different oxygen sensitivity of the two emissions. In the experiments described below, the ruthenium porphyrin phosphorescence is always obtained as the difference between the emission spectrum of the array in degassed and aerated solutions.

At the triplet level, the behavior of all the free-base systems is qualitatively similar. Upon excitation of **Fb(4)Ru** and **Fb(4)Ru$_4$** at 532 nm, where the light is predominantly absorbed (see above) by the ruthenium porphyrin(s), the phosphorescent emission of this unit is completely quenched (i.e. it is practically negligible by comparison with an optically

Table 1. Photophysical data on representative models and arrays.

	Fluorescence			Phosphorescence[a]			Transient absorption[b]	
	λ_{max} [nm][c]	τ [ns]	I_{rel}	λ_{max} [nm][c]	τ [μs][b]	I_{rel}[d]	λ_{max} [nm][c]	τ [μs]
Fb	653	9.7	1[e]	–	–	–	$\leq$440	800
Zn	609	2.4[f]	1[g]	–	–	–	470	900
Ru	–	–	–	726	$\approx$30	1	475	30
Fb(4)Ru	652	3.6	0.40[e]	[h]	[h]	$\leq$0.01	$\leq$440	540
Fb(4)Ru$_4$	653	$\approx$0.5	0.07[e]	[h]	[h]	$\leq$0.01	$\leq$440	650
Zn(4)Ru	600	[h]	0.30[g]	726	$\approx$70	0.30	470	110
Zn(4)Ru$_4$	[h]	[h]	$\leq$0.01[g]	726	$\approx$70	0.95	470	75

[a] From the difference spectrum between degassed and aerated solutions. [b] Degassed solution. [c] High-energy band. [d] Intensity, relative to optically matched (530 nm) solutions of **Ru**. [e] Intensity, relative to optically matched (588 nm) solutions of **Fb**. [f] From reference [36]. [g] Intensity, relative to optically matched (588 nm) solutions of **Zn**. [h] Too weak and/or too short-lived for detection.

0947-6539/99/0509-2674 $ 17.50+.50/0 *Chem. Eur. J.* **1999**, *5*, No. 9

matched solution of **Ru** (Table 1)). In transient absorption, the behavior of these arrays is also clear-cut: (i) the triplet–triplet spectrum characteristic of the ruthenium porphyrin moiety has completely disappeared, and is replaced by that of the free-base porphyrin (as shown in Figure 12 for **Fb(4)Ru**);

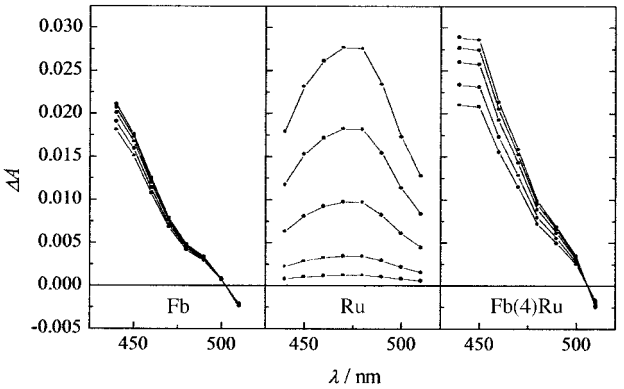

Figure 12. Transient absorption difference spectra of **Fb**, **Ru**, and **Fb(4)Ru**, obtained in laser flash photolysis. Delay times 0, 10, 25, 50, 75 μs, from upper to lower trace.

(ii) the time scale of the transient decay is much longer than that of **Ru**, and similar to that of **Fb** (Figure 13, Table 1). Thus, the emission and transient absorption experiments clearly demonstrate quenching of the ruthenium porphyrin triplet and sensitization of the free-base one. This provides strong evidence for the occurrence of efficient triplet energy transfer [Eq. (3)] in the systems (Figure 8). The energy transfer rate lies in the time scale of a few nanoseconds, as the spectral

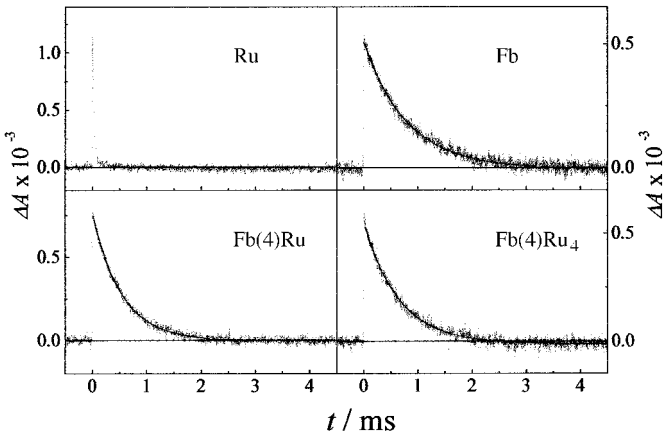

Figure 13. Transient decays of **Fb**, **Ru**, **Fb(4)Ru**, and **Fb(4)Ru$_4$**, under first-order conditions; deaerated solution in toluene, monitored at 460 nm (see text).

changes expected for this process can be detected in transient absorption within the laser pulse. The initial intensity of the transient spectral changes obtained in the laser flash photolysis of **Fb(4)Ru**, for example, is about the same as that obtained with an optically matched (at 532 nm) solution of **Fb**, which demonstrates that in the array *both* the ruthenium porphyrin intersystem crossing (Fb-^{1}*Ru →Fb-^{3}*Ru) and the triplet energy transfer process [Eq. (3)] are 100% efficient (Figure 8). Interestingly, the lifetime of the free-base triplet states in the **Fb(4)Ru** and **Fb(4)Ru$_4$** arrays (Table 1) is not substantially shortened with respect with that of the **Fb** model. The main deactivation process of the free-base triplet state is intersystem crossing to the ground state, ^{3}*Fb-Ru →^{1}Fb-Ru in Figure 8, and one could wonder why the heavy atom effect of ruthenium should be much weaker here than for the excited-state intersystem crossing process ^{1}*Fb-Ru →^{3}*Fb-Ru. This can be understood if, as suggested above, the Fb$^-$-Ru$^+$ charge transfer state is involved, via mixing into the local excited states, in the transmission of the spin-orbit perturbation between the units. For energy reasons, this mixing is much less effective on the ^{3}*Fb-Ru →^{1}Fb-Ru intersystem crossing process than on the ^{1}*Fb-Ru →^{3}*Fb-Ru process.

For all the zinc-substituted systems, the triplet excited-state behavior is qualitatively different from that of the free-base analogues. Upon excitation of **Zn(4)Ru** and **Zn(4)Ru$_4$** at 532 nm, with light predominantly absorbed by the ruthenium porphyrin component, the phosphorescent emission of ruthenium porphyrin (λ_{max} = 726 nm, Figure 2 f, g) is still clearly observed. Its intensity is always substantial (Table 1) with respect to optically matched solutions of **Ru.** In transient absorption, the typical behavior is that depicted in Figure 14 for **Zn(4)Ru**. In this case, the interpretation is not as obvious as in the free-base case, as the triplet–triplet absorption spectra of the zinc and ruthenium porphyrin units are very similar. On close examination of Figure 14, the band profile of

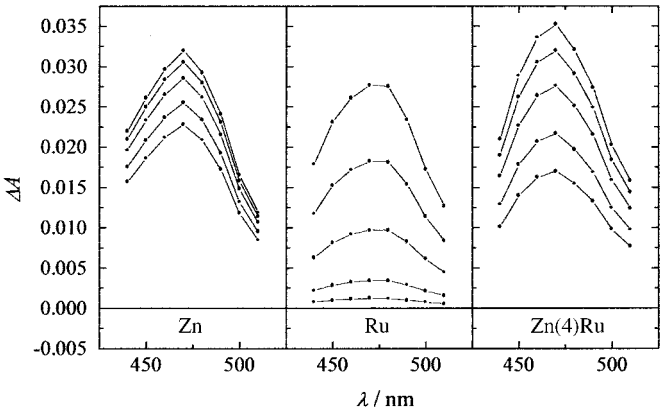

Figure 14. Transient absorption difference spectra of **Zn**, **Ru**, and **Zn(4)Ru** obtained in laser flash photolysis. Delay times 0, 10, 25, 50, 75 μs, from upper to lower trace.

the **Zn(4)Ru** transient seems to resemble more that of **Zn** (sharp peak at 470 nm) than that of **Ru** (broad maximum at 470–480 nm). It is important to note, on the other hand, that the time scale for the transient decays is much shorter than that of **Zn**, but definitely longer than that of **Ru** (Figure 15 and Table I). The simplest picture capable of accommodating these results is one in which the zinc porphyrin triplet, while remaining lower in energy, is sufficiently close to the ruthenium triplet as to allow equilibration between the states (Figure 9). In this hypothesis, the zinc porphyrin triplet is the main absorbing species in the transient experiments. At equilibrium, the ruthenium triplet states have a relatively small population but, because of the enhanced lifetime (relative to

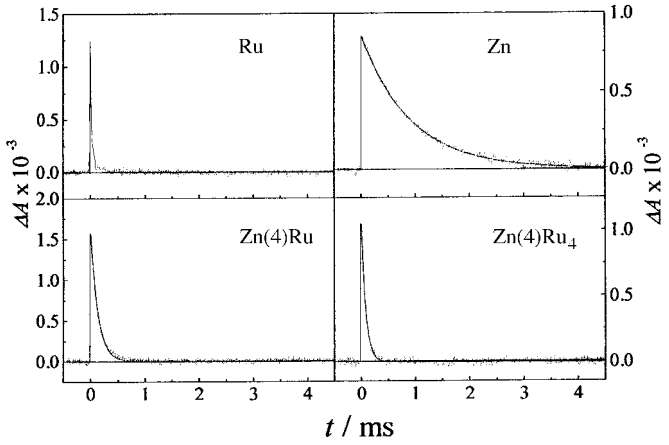

Figure 15. Transient decays of **Zn**, **Ru**, **Zn(4)Ru**, and **Zn(4)Ru$_4$**, under first-order conditions; deaerated solution in toluene, monitored at 460 nm (see text).

Ru), can give rise to relatively intense phosphorescent emission. In a standard two-state equilibrium model, the measurable parameters are related to the energy difference between the states, $\Delta E = (E_{Ru} - E_{Zn})$, by Equations (6) – (8).

$$\tau = (1+F_{Ru})\ \frac{\tau_{Ru}\tau_{Zn}}{\tau_{Ru} + \tau_{Zn}F_{Ru}} \quad (6)$$

$$I_{rel} = \left(\frac{F_{Ru}}{1+F_{Ru}}\right)\frac{\tau}{\tau_{Ru}} \quad (7)$$

$$F_{Ru} = n\ \exp\left(\frac{-\Delta E}{k_B T}\right) \quad (8)$$

In Equations (6) – (8), F_{Ru} is the Boltzmann population of the upper emitting state, n is the number of ruthenium porphyrin units, τ is the equilibrium lifetime common to both excited states, τ_{Ru} and τ_{Zn} are the intrinsic lifetimes of the isolated states (i.e. of monomeric models of the two units), and I_{rel} is the intensity of the ruthenium phosphorescence in the array relative to that of the monomeric model. For example, taking the values for τ_{Ru} and τ_{Zn} from the monomeric models and assuming a reasonable value of $\Delta E = 0.05$ eV, Equations (6) – (8) yield $I_{rel} = 0.95$ and $\tau = 80\ \mu s$ for **Zn(4)Ru$_4$**, in good agreement with the experimental findings (Table 1).

Strong additional support for this hypothesis for the equilibrium comes from the following experimental observations:

i) The lifetime of the ruthenium porphyrin phosphorescence in the arrays is about the same as that of zinc porphyrin triplet transient absorption (Table 1) (and is definitely *longer* than that of the **Ru** model).
ii) The efficiency of the ruthenium-based phosphorescence is almost independent of the excitation wavelength, irrespective of the nature of the light-absorbing chromophore (ruthenium or zinc porphyrin).
iii) Upon cooling to 77 K, the ruthenium-based emission completely disappears, while the red-shifted zinc porphyrin emission appears (see, for comparison, Figure 6).

Triplet energy transfer mechanism: The results presented above show that triplet – triplet energy transfer, either as an irreversible process (free-base systems) or as a reversible equilibration process (zinc porphyrin systems), is efficient in all the arrays. As to the mechanism, these energy transfer processes are no doubt of Dexter type, based on electron exchange.[46] In this section, we would like to point out some peculiarities of exchange energy transfer, as applied to chromophores in side-to-face geometry.

For efficient exchange interaction between a donor and an acceptor, the basic requirement is that of simultaneous HOMO – HOMO and LUMO – LUMO orbital overlap.[46, 47] If, for the sake of simplicity, the *meso* pyridyl group is considered to belong to the acceptor unit,[45, 48–50] attention should be focussed on orbital overlap between the pyridyl fragment and the ruthenium porphyrin ring. When the relevant orbitals are inspected, a fundamental symmetry mismatch becomes apparent. With respect to a twofold axis perpendicular to the ruthenium porphyrin,[51] both the HOMO and the LUMO on the pyridyl group, being π orbitals, are obviously antisymmetric (B symmetry in the C_2 point group). On the other hand, the HOMO and the LUMO of the ruthenium porphyrin ring[52] have opposite axial symmetries, which means that the LUMO is B (π) and the HOMO is A (σ) (Figure 16).[53–57] Thus, HOMO – HOMO overlap is zero by symmetry at the junction between the ruthenium porphyrin and the axial pyridyl group. In other words, through-bond exchange energy transfer is formally *symmetry forbidden* in this class of axially connected side-to-face porphyrin arrays. As usual for symmetry selection rules, it can be anticipated that both static distortions and vibronic coupling may lead to a substantial weakening of this prohibition. The actual occurrence of efficient triplet energy transfer can be explained along these lines. On the other hand, measurable consequences of this symmetry selection rule on the kinetics of energy transfer cannot be ruled out.

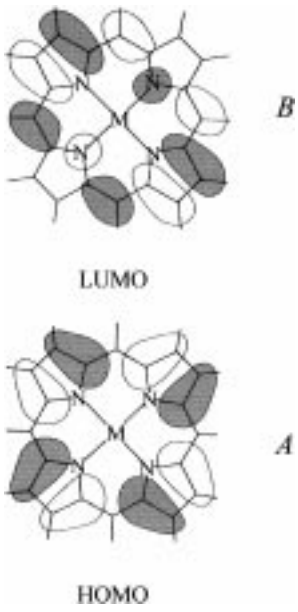

Figure 16. Schematic representation of the HOMO and LUMO of a metal porphyrin (adapted from ref. [52]). Symmetry labels are for a C_2 point group, with symmetry axis perpendicular to the porphyrin plane.

For experimental reasons, information on the kinetics of triplet energy transfer in the arrays studied is limited to the free-base systems. In such systems, the process can be observed (but not time-resolved) on a time scale comparable to that of the laser pulse. This implies rate constants in the range $10^8 - 10^9\ s^{-1}$. It is difficult to find meaningful touchstones for this result, as the literature on triplet energy transfer in porphyrin arrays is rather limited.[58, 59] Overall, considering the compact structure of the arrays[60] and the few data available on related, less compact systems,[61, 62] the triplet energy transfer processes observed in this work appear to be

0947-6539/99/0509-2676 $ 17.50+.50/0 *Chem. Eur. J.* **1999**, *5*, No. 9

somewhat slower than expected. At this stage, it is impossible to say whether the symmetry arguments discussed here are relevant to the experimental observations. To address this point, specific comparisons between systems with the same molecular components in different geometries (e.g. side-to-face vs laterally connected dimers) would be needed. These aspects will be further explored.

Conclusions

A detailed photophysical study has been carried out on a series of dimeric or pentameric side-to-face arrays, based on coordination of a free-base (or zinc-substituted) pyridylporphyrin to the metal center of one or more ruthenium porphyrin units. In all cases, the excited states of the ruthenium porphyrin units, both at the singlet and at the triplet level, are higher in energy than those of the axial free-base or zinc unit. In the photophysical behavior of the arrays, practically independent of their perpendicular or canted geometry, two main supramolecular features are observed. Firstly, the singlet state of the axial unit is strongly perturbed by the heavy-atom effect of the attached ruthenium units, which results in enhanced intersystem crossing and pronounced fluorescence quenching. Secondly, efficient energy transfer between the units takes place at the triplet level, which results in different types of behavior dependent on the nature of the substituted axial porphyrin. In the zinc porphyrin case, equilibrium between the triplet states of the two units is established prior to deactivation. In the free-base case, the result is irreversible quenching of the ruthenium porphyrin triplet and sensitization of the free-base triplet. On the basis of orbital overlap considerations, it is shown that exchange energy transfer is formally symmetry-forbidden in axially linked porphyrin arrays of this type. In practice, this selection rule may, to some extent, affect the rates, but is not strict enough as to prevent the occurrence of efficient energy transfer.

Experimental Section

Materials and procedures: The syntheses and NMR spectroscopic characterizations of the canted pentamers **Fb(3)Ru$_4$** and **Zn(3)Ru$_4$**, and dimers **Fb(3)Ru** and **Zn(3)Ru**, were reported in references [30a and b]. The synthetic procedures and NMR characterization of the products are reported here in detail. For the sake of brevity, some of these data were omitted from our previous publication on the corresponding perpendicular arrays **Fb(4)Ru, Zn(4)Ru, Fb(4)Ru$_4$**, and **Zn(4)Ru$_4$**.[28]

Fb(4)Ru: Addition of a slight excess of 4′MPyP (73 mg, 0.11 mmol) to a suspension of [Ru(TPP)(CO)(EtOH)] (81 mg, 0.1 mmol) in chloroform yielded a deep purple solution within minutes. The system was allowed to react overnight at room temperature. The crude product precipitated from the concentrated solution upon addition of *n*-hexane and was collected on a filter, washed with cold methanol and *n*-hexane, and vacuum dried; yield 100 mg (70%). M.p. $>300\,^{\circ}C$; ^1H NMR (400 MHz, $CDCl_3$, 25 °C, TMS): $\delta = 8.73$ (s, 8H, pyrrole TPP), 8.71 (m, 4H, pyrrole 4′MPyP), 8.46 (d, 2H, pyrrole 4′MPyP), 7.30 (d, 2H, pyrrole 4′MPyP), 8.07 (m, 2H, *o*-H of 4′MPyP phenyl *trans* to Ru), 8.00 (m, 4H, *o*-H of 4′MPyP phenyls *cis* to Ru), 8.32 (m, 4H, *exo o*-H of TPP phenyls), 8.18 (m, 4H, *endo o*-H of TPP phenyls),[63] 7.66–7.77 (m, 21H, *m*-H + *p*-H of TPP + 4′MPyP phenyls) 6.06 (m, 2H, 4′py H3,5), 1.94 (m, 2H, 4′py H2,6), −3.62 (s, 2H, NH); ^{13}C NMR (selected) (100.5 MHz, $CDCl_3$, 25 °C, TMS): $\delta = 180.2$ (CO); IR (selected) (Nujol): $\tilde{\nu} = 1950\ cm^{-1}$ (C=O); UV/Vis (toluene): λ_{max} (ε) = 417 (480000), 519 (27000), 531 (23000), 590 (6300), 648 nm (4000).

Fb(4)Ru$_4$: A synthetic procedure analogous to that reported above for the dimer **Fb(4)Ru** was followed (yield 70%). M.p. $>300\,^{\circ}C$; ^1H NMR (400 MHz, $CDCl_3$, 25 °C, TMS): $\delta = 8.67$ (s, 32H, pyrrole TPP), 8.28 (m, 16H, *exo o*-H of TPP phenyls), 7.99 (m, 16H, *endo o*-H of TPP phenyls), 7.76 (m, 32H, *exo m*-H + *p*-H of TPP phenyls), 7.57 (m, 16H, *endo m*-H of TPP phenyls), 6.68 (s, 8H, pyrrole 4′TPyP), 5.51 (m, 8H, 4′py H3,5), 1.72 (m, 8H, 4′py H2,6), −4.78 (s, 2H, NH); ^{13}C NMR (selected) (100.5 MHz, $CDCl_3$, 25 °C, TMS): $\delta = 180.1$ (CO); IR (selected) (Nujol): $\tilde{\nu} = 1952\ cm^{-1}$ (C=O); UV/Vis (toluene): λ_{max} (ε) = 409 (1250000), 530 (74600), 566 (18500), 588 (11500), 649 nm (4200).

Zn(4)Ru: A solution of zinc acetate (54 mg, 0.25 mmol) in methanol (3 mL) was added to the deep purple solution of **Fb(4)Ru** (70 mg, 4.9×10^{-2} mmol) in chloroform (7 mL). The system was allowed to react overnight at room temperature. The crude product precipitated spontaneously from the concentrated solution and was collected on a filter, thoroughly washed with methanol and then with *n*-hexane, and vacuum dried; yield 58 mg (80%). M.p. $>300\,^{\circ}C$; ^1H NMR (400 MHz, $CDCl_3$, 25 °C, TMS): $\delta = 8.73$ (s, 8H, pyrrole TPP), 8.81 (m, 4H, pyrrole 4′MPyP), 8.56 (d, 2H, pyrrole 4′MPyP), 7.39 (d, 2H, pyrrole 4′MPyP), 8.08 (m, 2H, *o*-H of 4′MPyP phenyl *trans* to Ru), 8.00 (m, 4H, *o*-H of 4′MPyP phenyls *cis* to Ru), 8.32 (m, 4H, *exo o*-H of TPP phenyls), 8.18 (m, 4H, *endo o*-H of TPP phenyls), 7.66–7.77 (m, 21H, *m*-H + *p*-H of TPP + 4′MPyP phenyls), 6.05 (m, 2H, 4′py H3,5), 1.93 (m, 2H, 4′py H2,6); ^{13}C NMR (selected) (100.5 MHz, $CDCl_3$, 25 °C, TMS): $\delta = 180.1$ (CO); IR (selected) (Nujol): $\tilde{\nu} = 1949\ cm^{-1}$ (C=O); UV/Vis (toluene): λ_{max} (ε) = 413 (411600), 423 (446700), 530 (23000), 547 (26200), 589 (5700), 652 nm (9600).

Zn(4)Ru$_4$: A synthetic procedure analogous to that reported above for the dimer **Zn(4)Ru** was followed (yield 70%). M.p. $>300\,^{\circ}C$; ^1H NMR (400 MHz, $CDCl_3$, 25 °C, TMS): $\delta = 8.67$ (s, 32H, pyrrole TPP), 8.28 (m, 16H, *exo o*-H of TPP phenyls), 7.99 (m, 16H, *endo o*-H of TPP phenyls), 7.77 (m, 32H, *exo m*-H + *p*-H of TPP phenyls), 7.54 (m, 16H, *endo m*-H of TPP phenyls), 6.77 (s, 8H, pyrrole 4′TPyP), 5.51 (m, 8H, 4′py H3,5), 1.71 (m, 8H, 4′py H2,6); IR (selected) (Nujol): $\tilde{\nu} = 1951\ cm^{-1}$ (C=O); UV/Vis (toluene): λ_{max} (ε) = 409 (1190000), 532 (66000), 555 (35400, sh), 592 nm (9100).

Spectroscopic and electrochemical measurements: The solvents for the spectroscopic measurements, dimethylformamide (DMF), chloroform ($CHCl_3$), dichloromethane (CH_2Cl_2), ethanol (EtOH), methanol (MeOH), methylcyclohexane, and toluene, were of spectroscopic grade and used as received. The solutions used in the photochemical experiments were degassed with *at least five* freeze-pump-thaw cycles and subsequently sealed under vacuum ($P = 4 \times 10^{-6}$ Pa). The recording of excitation spectra was complicated by the dual requirements of optically diluted solutions and an array concentration that lies within the tested stability range. The problem was solved by the use of 1×10^{-5} M solutions and 1 mm cells in a 45° excitation-emission geometry. Cyclic voltammetric measurements (CV) were carried out on argon-purged 10^{-3} M sample solutions in CH_2Cl_2 (Romil, Hi-dry), containing $[TBA]PF_6$ (0.1 M, Fluka, electrochemical grade, 99%; oven-dried). A conventional three-electrode cell assembly was used for the CV measurements: a saturated calomel electrode (SCE, ∅ = 6 mm, AMEL) and a platinum wire, both separated from the test solution by a frit, were used as reference and counter electrode, respectively; a glassy carbon electrode (8 mm^2, AMEL) was used as a working electrode. Cyclic voltammograms were recorded at different scan rates in the range 50–500 $mV\,s^{-1}$ at room temperature.

Apparatus: UV/Vis spectra were recorded with a Kontron Uvikon 860 or a Perkin Elmer LAMBDA40 spectrophotometer. Emission spectra were taken on a Perkin Elmer MPF44E or on a Spex Fluoromax-2 spectrofluorimeter, equipped with Hamamatsu R3896 tubes. The emission spectra were corrected for the instrumental response by calibration with an NBS standard quartz-halogen lamp. ^1H and ^{13}C NMR experiments were performed in $CDCl_3$ at 400 and 100.5 MHz, on a Jeol EX400 spectrometer. Nanosecond flash photolysis was performed by irradiating the sample with 6–8 ns (fwhm) pulses of a Continuum Surelight II Nd:Yag laser (10 Hz repetition rate) and using a pulsed Xe lamp perpendicular to the laser beam as probing light. The desired excitation wavelength was obtained by frequency doubling (532 nm). The 150 W Xe lamp was equipped with an

Applied Photophysics Model 40 power supply and Applied Photophysics Model 410 pulsing unit (2 ms pulses). A shutter, Oriel Model 71445, placed between the lamp and the sample was opened for 100 ms to prevent PMT fatigue and photodecomposition. Suitable pre- and post-cutoff and bandpass filters were used to prevent photodecomposition, and scattered light from the laser. The light was collected in a LDC Analytical monochromator, detected by a R928 PTM (Hamamatsu), and recorded on a Lecroy 9360 (600 MHz) oscilloscope. The laser oscillator, Q-switch, lamp, shutter, and trigger were externally controlled with a digital logic circuit, which allowed for synchronous timing. The absorption transient decays were plotted as $\Delta A = \log(I_o/I_t)$ vs. time, where I_o was the monitoring light intensity prior the laser pulse and I_t was the observed signal at delay time t. Transient spectra were obtained from the decays measured at various wavelengths, by sampling the absorbance changes at constant delay time. Emission lifetimes in the microsecond time range were measured with the same laser/monochromator/phototube setup used for the flash photolysis experiments. Emission lifetimes in the nanosecond time range were measured by time-correlated, single-photon counting with a PRA 3000 nanosecond fluorescence spectrometer equipped with a Model 510B nanosecond pulsed lamp and a Model 1551 cooled photomultiplier; the data were collected on a Tracor Northern multichannel analyzer and processed with the original Edinburgh Instruments software. Electrochemical measurements were carried out with an AMEL 552 potentiostat, an AMEL 568 programmable function generator, an AMEL 560/a interface and an AMEL Model 863 X/Y recorder. All the low-temperature experiments were measured on an Oxford Instruments DN 704 cryostatic equipment with quartz windows and a standard 1 cm spectrofluorimetric cuvette.

Acknowledgments

This work was carried out with financial support from MURST (Progetto Dispositivi Supramolecolari), CNR (Centro di Fotoreattività e Catalisi, Ferrara), and EEC (TMRX-CT96-0076).

[1] *The Porphyrins*, *vols. 1–5* (Ed.: D. Dolphin), Academic Press, New York, **1978**.
[2] *Comprehensive Supramolecular Chemistry*, (Eds.: J. L. Atwood, J. E. Davies, D. D. MacNicol, F. Vögtle), Pergamon, Oxford, **1996**; J.-M. Lehn, *Supramolecular Chemistry: Concepts and Perspectives*, WCH, Weinheim, **1995**.
[3] a) V. Balzani, F. Scandola, *Supramolecular Photochemistry*, Horwood, Chichester, UK, **1991**; b) V. Balzani, F. Scandola in *Comprehensive Supramolecular Chemistry*, *vol. 10* (Eds.: J. L. Atwood, J. E. D. Davies, D. D. MacNicol, F. Vögtle, D. N. Reinhoudt), Pergamon, Oxford, **1996**, p. 687.
[4] J. Deisenhofer, O. Epp, K. Miki, R. Huber, H. Michel, *J. Mol. Biol.* **1984**, *180*, 385.
[5] C.-H. Chang, D. M. Tiede, J. Tang, U. Smith, J. Norris, M. Schiffer, *FEBS Lett.* **1986**, *205*, 82.
[6] J. P. Allen, G. Feher, T. O. Yeates, H. Komiya, D. C. Rees, *Proc. Natl. Acad. Sci. USA* **1987**, *84*, 5730.
[7] J. Deisenhofer, H. Michel, *Angew. Chem.* **1989**, *100*, 872, *Angew. Chem. Int. Ed. Engl.* **1989**, *28*, 829.
[8] R. Huber, *Angew. Chem.* **1989**, *100*, 849, *Angew. Chem. Int. Ed. Engl.* **1989**, *28*, 848.
[9] M. R. Wasielewski, *Chem. Rev.* **1992**, *92*, 435.
[10] A. Harriman, J. P. Sauvage, *Chem. Soc. Rev.* **1996**, 41.
[11] D. Gust, T. A. Moore, A. L. Moore, *Acc. Chem. Res.* **1993**, *26*, 198.
[12] G. McDermott, S. M. Prince, A. A. Freer, A. M. Hawthornthwaite-Lawless, M. Z. Papiz, R. J. Cogdell, N. W. Isaacs, *Nature* **1995**, *374*, 517.
[13] W. Kuhlbrandt, *Nature* **1995**, *374*, 497.
[14] S. Karrasch, P. A. Bullough, R. Ghosh, *EMBO J.* **1995**, *14*, 631.
[15] W. Kuhlbrandt, D. N. Wang, Y. Fujiyoshi, *Nature*, **1994**, *367*, 1994.
[16] a) J. P. Collman, J. T. McDevitt, C. R. Leidner, G. T. Yee, J. B. Torrance, W. A. Little, *J. Am. Chem. Soc.* **1987**, *109*, 4606; b) V. Marvaud, J.-P. Launay, *Inorg. Chem.* **1993**, *32*, 1376; c) M. Ikonen, D. Guez, V. Marvaud, D. Markovitsi, *Chem. Phys. Lett.* **1994**, *231*, 93.
[17] H. L. Anderson, *Inorg. Chem.* **1994**, *33*, 972.
[18] a) C. J. Walter, H. L. Anderson, J. K. M. Sanders, *J. Chem. Soc. Chem. Commun.* **1993**, 458; b) X. Chi, A. J. Guerin, R. A. Haycock, C. A. Hunter, L. D. Sarson, *J. Chem. Soc. Chem. Commun.* **1995**, 2567; c) S. Anderson, H. L. Anderson, A. Bashall, M. McPartlin, J. K. M. Sanders, *Angew. Chem.* **1995**, *106*, 1196, *Angew. Chem. Int. Ed. Engl.* **1995**, *34*, 1096; d) A. Vidal-Ferran, N. Bampos, J. K. M. Sanders, *Inorg. Chem.* **1997**, *36*, 6117; e) P. N. Taylor, A. P. Wylie, J. Huuskonen, H. L. Anderson, *Angew. Chem.* **1998**, *110*, 1033, *Angew. Chem. Int. Ed.* **1998**, *37*, 986; f) C. C. Mak, N. Bampos, J. K. M. Sanders, *Angew. Chem.* **1998**, *110*, 3169, *Angew. Chem. Int. Ed.* **1998**, *37*, 3020.
[19] a) C. M. Drain, J.-M. Lehn, *J. Chem. Soc. Chem. Commun.* **1994**, 2313; b) H. Yuan, L. Thomas, L. K. Woo, *Inorg. Chem.* **1996**, *35*, 2808; c) R. V. Slone, J. T. Hupp, *Inorg. Chem.* **1997**, *36*, 5422; d) P. J. Stang, J. Fan, B. Olenyuk, *Chem. Commun.* **1997**, 1453; e) C. M. Drain, F. Nifiatis, A. Vasenko, J. D. Batteas, *Angew. Chem.* **1998**, *110*, 2478, *Angew. Chem. Int. Ed.* **1998**, *37*, 2344.
[20] D. L Officer, A. K. Burrel, D. C. W. Reid, *Chem. Commun.* **1996**, 1657.
[21] M. J. Crossley, P. L. Burn, *J. Chem. Soc. Chem. Commun.* **1991**, 1569.
[22] a) R. W. Wagner, J. S. Lindsey, *J. Am. Chem. Soc.* **1994**, *116*, 9759; b) R. W. Wagner, J. S. Lindsey, J. Seth, V. Palaniappan, D. F. Bocian, *J. Am. Chem. Soc.* **1996**, *118*, 3996.
[23] J. L. Sessler, V. L. Capuano, A. Harriman, *J. Am. Chem. Soc.* **1993**, *115*, 4618.
[24] J. Davila, A. Harriman, L. R. Milgrom, *Chem. Phys. Lett.* **1987**, *136*, 427.
[25] a) S. Prathapan, T. E. Johnson, J. S. Lindsey, *J. Am. Chem. Soc.* **1993**, *115*, 7519; b) J.-S. Hsiao, B. P. Krueger, R. W. Wagner, T. E. Johnson, J. K. Delaney, D. C. Mauzerall, G. R. Fleming, J. S. Lindsey, D. F. Bocian, R. J. Donohoe, *J. Am. Chem. Soc.* **1996**, *118*, 11181.
[26] T. E. Clement, D. J. Nurco, K. M. Smith, *Inorg. Chem.* **1998**, *37*, 1150.
[27] A. Nakano, A. Osuka, I. Yamazaki, T. Yamazaki, Y. Nishimura, *Angew. Chem.* **1998**, *110*, 3172, *Angew. Chem. Int. Ed.* **1998**, *37*, 3023.
[28] E. Alessio, M. Macchi, S. Heath, L. G. Marzilli, *Chem. Commun.* **1996**, 1411.
[29] Abbreviations: TPP = 5,10,15,20-tetraphenylporphyrin; 4′MPyP = 5-(4′-pyridyl)-10,15,20-triphenylporphyrin; 4′TPyP = 5,10,15,20-tetra-(4′-pyridyl)porphyrin; 3′MPyP = 5-(3′-pyridyl)-10,15,20-triphenylporphyrin; 3′TPyP = 5,10,15,20-tetra(3′-pyridyl)porphyrin.
[30] E. Alessio, S. Geremia, S. Mestroni, T. Gianferrara, M. Slouf, A. Prodi, *Inorg. Chem.* **1999**, *38*, 2527–2529; E. Alessio, S. Geremia, S. Mestroni, E. Iengo, I. Srnova, M. Slouf, *Inorg. Chem.* **1999**, *38*, 869–875.
[31] a) N. Kariya, T. Imamura, Y. Sasaki, *Inorg. Chem*, **1997**, *36*, 833; b) K. Funatsu, A. Kimura, T. Imamura, A. Ichimura, Y. Sasaki, *Inorg. Chem*, **1997**, *36*, 1625; c) N. Kariya, T. Imamura, Y. Sasaki, *Inorg. Chem*, **1998**, *37*, 1658; d) K. Funatsu, T. Imamura, A. Ichimura, Y. Sasaki, *Inorg. Chem*, **1998**, *37*, 1798.
[32] L. M. A. Levine, D. Holten, *J. Phys. Chem.* **1988**, *92*, 714.
[33] a) E. Fleischer, A. M. Shachter, *Inorg. Chem.* **1991**, *30*, 3763; b) R. K. Kumar, I. Goldberg, *Angew. Chem.* **1998**, *110*, 3176, *Angew. Chem. Int. Ed.* **1998**, *37*, 3027.
[34] We thank a referee for pointing out this problem in an early version of this paper.
[35] K. M. Kadish, D. Chang, *Inorg. Chem.* **1982**, *21*, 3614.
[36] K. Kalyanasundaram, *Photochemistry of Polypyridine and Porphyrin Complexes*, Academic Press, London, **1992**.
[37] The fluorescent emission in quenched by about 5% in going from degassed to aerated solution. This small effect does not arise from diffusional quenching of the singlet state by oxygen (it is roughly the same for Fb and Zn, despite the strong difference in singlet lifetime and is not accompanied by a parallel lifetime quenching). It most likely corresponds to the quenching of a small amount of delayed fluorescence, ref. [36], arising from repopulation of the singlet after intersystem crossing to the (oxygen sensitive) triplet.
[38] K. Kalyanasundaram, *Inorg. Chem.* **1984**, *23*, 2453.
[39] The general integrated expression for transient spectral changes decaying by competing first- and second-order processes is $A_t = \frac{k_1 A_0}{(k_1 + k_2 A_0)e^{k_1 t} - k_2^{app} A_0}$, where A_t and A_0 are measured absorbance values at time t and time 0, k_1 is the first-order rate constant, and k_2^{app} is an apparent second-order rate constant, related to the true rate

  0947-6539/99/0509-2678 $ 17.50+.50/0

constant *by* $k_2 = k_2^{app}\Delta\varepsilon\ l$, where l is the effective optical cell length (0.6 cm in the experimental conditions used) and $\Delta\varepsilon$ is the molar absorptivity change. Satisfactory fits of the experimental decays to this equation were obtained (see Figure 4), with values of k_1 and k_2 reasonably constant as a function of laser power. The k_2 value was in the range $2 \pm 0.5 \times 10^9\ \text{M}^{-1}\text{s}^{-1}$ for all the monomeric models studied.

[40] G. M. Brown, F. R. Hopf, J. A. Ferguson, T. J. Meyer, D. G. Whitten, *J. Am. Chem. Soc*. **1973**, *95*, 5939.

[41] R. H. Felton in *The Porphyrins*, *vol. 5* (Ed.: D. Dolphin), Academic Press, New York, **1978**, p. 53.

[42] In a covalently linked donor–acceptor system, both covalent and electrostatic factors may alter the energy of the charge transfer state with respect to the simple algebraic sum of the redox potentials of the units. Given the weakly coupled nature of these supramolecular systems, covalent corrections are likely to be negligible in this case. The electrostatic work term can be accounted for by the use of standard expressions, ref. [43].

[43] D. Rehm, A. Weller, *Ber. Bunseges. Phys. Chem*. **1969**, *73*, 834; A. Weller, *Z. Phys. Chem.* 1982, *133*, 93.

[44] D. Gust, T. A. Moore, A. Moore, F. Gao, D. Luttrull, J. M. DeGraziano, X. C. Ma, L. R. Makings, S-J. Lee, R. V. Bensasson, M. Rougée, F. C. De Schryver, M. Van der Auweraer, *J. Am. Chem. Soc*. **1991**, *113*, 3638.

[45] H. E. Toma, K. Araki, *J. Photochem. Photobiol. A: Chem*. **1994**, *83*, 245.

[46] D. L. Dexter, *J. Chem. Phys*. **1953**, *21*, 836.

[47] G. L. Closs, M. D. Johnson, J. R. Miller, P. Piotrowiak, *J. Am. Chem. Soc.* **1989**, *111*, 3751.

[48] To be more precise, the *meso* pyridyl group should be considered as an individual electronic subsystem, and its coupling with the acceptor porphyrin should be explicitly included in the picture. At the junction between the *meso* pyridyl group and the acceptor porphyrin, orbital overlap depends on the dihedral angle, and is zero only for an exact orthogonal geometry. In the solid state, dihedral angles of ca. 65° and 60° have been measured in Zn(3)Ru_4[30] and Fb(3)Ru[30], respectively. Experimentally, electron transfer[9,49] and triplet energy transfer[45, 50] have been found to take place efficiently across a variety of similarly twisted connecting groups.

[49] M. T. Indelli, F. Scandola, L. Flamigni, J.-P. Collin, J.-P. Sauvage, A. Sour, *Inorg. Chem*. **1997**, *36*, 4247.

[50] J.-P. Sauvage, J.-P. Collin, J.-C. Chambron, S. Guillerez, C. Coudret, V. Balzani, F. Barigelletti, L. De Cola, L. Flamigni, *Chem. Rev.*, **1994**, *94*, 993.

[51] This is a true symmetry axis only for the perpendicular arrays. It could also be considered for the canted arrays to describe the local symmetry of the axial junction.

[52] D. Spangler, G. M. Maggiora, L. L. Shipman, R. E. Chirtoffersen, *J. Am. Chem. Soc*. **1977**, *99*, 7478.

[53] Two additional orbitals (LUMO + 1 and HOMO − 1, lying very close to LUMO and HOMO) are usually relevant to porphyrin spectroscopy (four-orbital model[54]). Their nodal properties and symmetry behavior with respect to axial C_2 are the same as those of the HOMO and LUMO shown in Figure 16. [55]

[54] M. Gouterman in *The Porphyrins*, *vol. 3* (Ed.: D. Dolphin), Academic Press, New York, **1978**, Chapter 1.

[55] This feature is common to cyclic π-systems. If the π electrons are considered as being confined to a one-dimensional ring[56] the wavefunctions are of the form $\exp(\pm im\phi)$, exhibiting $2m$ radial nodes and alternate symmetric–antisymmetric behavior with respect to a C_2 axis perpendicular to the ring. As the HOMO and LUMO differ in m by one unit ($m = 4, 5$ in the case of porphyrins,[56, 57] cyclic systems with $\pi-\pi^*$ excited states cannot generally meet the overlap conditions required for undergoing Dexter energy transfer from an axial π-π* chromophore.

[56] W. T. Simpson, *J. Chem. Phys.* **1949**, *17*, 1218.

[57] R. Cave, P. Siders, R. A. Marcus, *J. Phys. Chem*. **1986**, *90*, 1436.

[58] For this process to be effective following direct excitation, the presence of a heavy metal (on the porphyrin with the highest energy levels) is essential. In fact, unless intersystem crossing is exceedingly fast, energy transfer at the singlet level will prevent the occurrence of any triplet pathway. This requisite can be circumvented, in favorable cases, by studying triplet energy transfer after indirect excitation with an external triplet energy donor.[59]

[59] H. Levanon, A. Regev, P. K. Das, *J. Phys. Chem.* **1987**, *91*, 14.

[60] In the perpendicular and canted arrays, respectively, the center-to-center distances are about 9.8 and 8.6 Å, and the number of bonds intervening between the porphyrin rings is six and five.

[61] The closest example is that of the oblique bisporphyrins investigated by Brun et al.,[62] where an Au^{III} poprhyrin and a free-base or a zinc porphyrin are connected in the meso positions by a 2,9-phenyl-1,10-phenathroline spacer. Triplet energy transfer was observed to occur from the gold(III) porphyrin to the free-base and zinc units with rate constants of $7.0 \times 10^9\ \text{s}^{-1}$ and/or $1.2 \times 10^9\ \text{s}^{-1}$, respectively. In these systems, the center-to-center distance was about 13.6 Å and the through-bond pathway between the porphyrin rings involved 15 bonds.

[62] A. Brun, A. Harriman, V. Heitz, J-P. Sauvage, *J. Am. Chem. Soc*. **1991**, *113*, 8657.

[63] The phenyl rings on TPP are hindered with respect to rotation about the C(*meso*)–C(phenyl) bond and are nearly perpendicular to the Ru(TPP) mean plane. Therefore the *ortho* and *meta* protons on one side of each phenyl ring (*endo*-H) fall into the anisotropic region of the perpendicular pyridylporphyrin and experience its shielding effect; their resonances are consequently shifted upfield compared to those of the corresponding *exo* protons.

Received: August 3, 1998
Revised version: March 16, 1999 [F 1281]